Evaluation of the Bioavailability and Metabolism of Nitroderivatives of Hydroxytyrosol Using Caco-2 and HepG2 Human Cell Models

Elena **Gallardo**[1,2,3], Beatriz **Sarria**[1], José Luis **Espartero**[2], José Antonio **Gonzalez Correa**[3], Laura **Bravo-Clemente**[1], Raquel **Mateos**[1*]

[1]Department of Metabolism and Nutrition, Institute of Food Science, Technology and Nutrition (ICTAN), CSIC, Madrid, Spain; [2]Department of Organic and Pharmaceutical Chemistry, Faculty of Pharmacy, University of Seville, Spain; [3]Department of Pharmacology and Therapeutics, School of Medicine, University of Malaga.

Running title: Evaluation of the bioavailability and metabolism of nitroderivatives of hydroxytyrosol

*Corresponding author:

Raquel Mateos Briz (raquel.mateos@ictan.csic.es)

Department of Metabolism and Nutrition

Institute of Food Science, Technology and Nutrition (ICTAN-CSIC). Spanish National Research Council (CSIC). C/ José Antonio Nováis 10, 28040 Madrid, Spain.

Tel. +34.915492300

Fax: +34.915493627

Abstract

Considering that nitrocatechols present putative effect against Parkinson Disease, the absorption and metabolism of nitroderivatives of hydroxytyrosol (HT) were assessed using human cell model systems. The test compounds nitrohydroxytyrosol (NO_2HT), nitrohydroxytyrosyl acetate (NO_2HT-A), and ethyl nitrohydroxytyrosyl ether (NO_2HT-E) were efficiently transferred across human Caco-2 cell monolayers as an intestinal barrier model, being NO_2HT-A and NO_2HT-E better ($p<0.05$) absorbed (absorption rate (AR) = 1.4 ± 0.1 and 1.5 ± 0.2, respectively) than their precursor, NO_2HT (AR = 1.1 ± 0.1). A significant amount of the absorbed compounds remained unconjugated (81%, 70% and 33% for NO_2HT, NO_2HT-A and NO_2HT-E, respectively) after incubation in Caco-2 cells, being available for hepatic metabolism. Nitrocatechols were extensively uptaken and metabolized by human hepatoma HepG2 cells as a model of the human liver. Both studies revealed extensive hydrolysis of NO_2HT-A into NO_2HT, while NO_2HT-E was not hydrolyzed. Glucuronide (75-55%), methylglucuronide (25-33%) and methyl derivatives (0-12%) were the main nitrocatechol metabolites detected after metabolism Caco-2 and HepG2 cells. In conclusion, NO_2HT, NO_2HT-A and NO_2HT-E show high in vitro bioavailability and are extensively metabolized by hepatic cells.

Keywords: nitrocatechols, hydroxytyrosol, bioavailability, metabolism, Parkinson Disease

Introduction

Given the current ageing of the population in developed countries, the prevalence of dementia will approximately double every 20 years, reaching 115 million by 2050.[1] As part of the normal ageing process, cognitive function degenerates and the risk of suffering a range of inflammatory neurodegenerative conditions increases. Parkinson's disease (PD) is a multisystem neurodegenerative disorder which afflicts nearly 1% of the population above the age of 60. The main feature of PD is the progressive loss of midbrain dopamine (DA) neurons, with resulting dopaminergic deafferentiation of the basal ganglia, which gives rise to characteristic motor disturbances that include slowing of movement, muscular rigidity, and resting tremor. Recovery of DA levels has constituted the classical symptomatic treatment against PD. L-DOPA (3,4-dihydroxyphenyl-L-alanine) has been widely used as a drug for PD in combination with catechol *O*-methyltransferase (COMT) inhibitors, being COMT an enzyme involved in the degradation of dopamine.[2,3] During the 90s, two COMT inhibitors, entacapone and tolcapone, were developed and included into the clinical treatment of PD. Both compounds present a nitrocatechol moiety in their structures, which has shown to be essential for the inhibitory activity. However, the use of tolcapone has been restricted due to its hepatotoxicity,[2] whereas entacapone has shown to present a short lifetime requiring high doses to be effective; in addition, its hydrophilic nature may compromise its absorption though the blood brain barrier (BBB).[4] Therefore, some studies have focused on obtaining new COMT inhibitors.[5]

Based on the broad biological activity that natural olive oil phenols hydroxytyrosol (HT) and hydroxytyrosyl acetate (HT-A) have shown,[6-8] their nitroderivated compounds nitrohydroxytyrosol (NO_2HT) and nitrohydroxytyrosyl acetate (NO_2HT-A) (Figure 1), have been synthesized[9] in order to increase the assortment of compounds with potential therapeutic properties against PD. Additionally, another nitroderivative compound was also synthesized,[10] ethyl nitrohydroxytyrosyl ether (NO_2HT-E) (Figure 1), due to the high bioavailability of its

precursor ethyl hydroxytyrosyl ether (HT-E) in Caco-2 cells[11] and HepG2 cells,[12] and its notable protective effects against oxidative stress.[13] Recent experiments have shown that NO_2HT, NO_2HT-A and NO_2HT-E have remarkable inhibitory effects on COMT activity in the brain after both acute and chronic systemic treatments.[14] Furthermore, using a microdialysis intracerebral administration technique, an extended in vivo COMT inhibitory activity has been observed in keeping with the lipophilic nature of the tested nitroderivatives[15] and other novel COMT inhibitor compounds.[5,16,17] Likewise, nitroderivatives of HT are also able to protect against oxidative stress,[18] which is likely to be involved in neurodegenerative disorders such as PD.

Since in vivo biological activity of polyphenols depends on their intestinal uptake and metabolism, the absorption of the nitrocatechols and the extent to which they are conjugated and metabolized has been investigated in Caco-2 cells, a cellular line recognized by the Food and Drug Administration[19] as the most suitable experimental model for intestinal permeability and transport studies, being widely utilized for toxicological and pharmacological studies.

Moreover, in order to understand the biotransformation of these compounds and to evaluate the stability of the nitrocatechol moiety, which plays a key role in the inhibitory COMT activity, the metabolism of nitroderivatives of hydroxytyrosol has also been evaluated in human hepatoma cells (HepG2), considered one of the most reliable experimental models to study the metabolism of xenobiotics.[20]

Materials and methods

Chemicals

Acetonitrile, formic acid, sodium chloride, disodium hydrogen phosphate anhydrous, potassium dihydrogen phosphate, phenolsulfonphthalein (phenol red), and ascorbic acid were acquired from Panreac (Barcelona, Spain). Antibiotics (gentamicin, penicillin, and streptomycin), enzymes (catechol-*O*-methyltransferase, β-glucuronidase/sulfatase), *S*-adenosyl-*L*-methionine chloride, UDP-glucuronic acid, non-essential amino acids and dimethyl

sulfoxide were purchased from Sigma Chemical Co. (Madrid, Spain). Media, trypsine and fetal bovine serum (FBS) were from Biowhitaker (Innogenetics, Madrid, Spain). All reagents were of analytical or chromatographic grade. Hydroxytyrosol (HT) was recovered with 95% purity from olive oil wastewaters.[21] Nitrohydroxytyrosol (NO_2HT), nitrohydroxytyrosyl acetate (NO_2HT-A) and ethyl nitrohydroxytyrosyl ether (NO_2HT-E) were prepared from free HT, isolated from olive oil wastewaters, as described elsewhere.[9,10]

Cell cultures and treatments

The human colon adenocarcinoma cell line Caco-2 was obtained from Scientific Instrument Center at University of Granada (Spain) and cultured between passages 48 and 52. Cells were grown in Dulbecco Modified Eagle´s Medium (DMEM-21063) supplemented with 10% (v/v) fetal bovine serum (FBS), 1% (v/v) non-essential amino acids, 10.000 U/mL penicillin and 1000 μg/mL streptomycin, in a humidified atmosphere of 5% CO_2 and 95% air at 37°C.

The human hepatoma cell line HepG2 cells was a kind gift from Dr Paloma Martin-Sanz (Instituto de Bioquímica, CSIC, Madrid, Spain). Cells were grown in DMEM-F12 medium supplemented with 2.5% (v/v) FBS and 50 mg/L of each gentamicin, penicillin and streptomycin in a humidified incubator containing 5% CO_2 and 95% air at 37°C.

To prevent any potential interference between serum components and the test phenolic compounds, Caco-2 and HepG2 cells were changed to serum-free medium before developing the metabolism experiments. A control without test compound was used in all experiments. After finishing the incubations, media and cells were processed as follows: media was collected and stored at -20°C until analysis. Cells were washed twice with PBS (0.01 M phosphate buffered saline solution, pH 7.4) and harvested by scraping. Cells from replicate plates or wells corresponding to a particular condition were combined in an eppendorf vial. After centrifugation at 1250 rpm for 5 min at 4°C, supernatants were removed and the cell pellets

resuspended in 200 μL of PBS. Cells were sonicated for 10 min at room temperature and centrifuged at 7000 rpm for 10 min at 4°C. Supernatants were kept frozen at -20°C.

Stability evaluation and cytotoxic effect of test solutions

Standard stock solutions (10 mM) were prepared in 10% DMSO in deionized water, diluted with deionized water to get 1000 μM (1% of DMSO) concentration, and ultimately diluted with serum-free medium supplemented with 500 μM ascorbic acid to obtain 100 μM (0.1% DMSO) test solutions. Stability of nitrocatechols dissolved in serum-free medium or in medium supplemented with 300, 500 and 1000 μM ascorbic acid was monitored at 37°C for 24 h.

On the other hand, potential cellular damage induced by these phenolic compounds was assessed by the crystal violet assay as described by Sarria et al.[18] Test solutions (100 μM) of each nitrocatechol were assessed in both cell lines (Caco-2 and HepG2) in comparison with a control consisting in serum-free medium supplemented with 500 μM ascorbic acid and 0.1% DMSO.

Transport and metabolism experiments in Caco-2 cells

Caco-2 cells were grown in DMEM-21063 medium in Transwell inserts with semipermeable membrane coated with type I collagen (24 mm diameter, 4.67 cm^2 area and 0.4 μm pore size, Corning Costar, NY). Cells were seeded at a density of 40 x 10^4 cells per cm^2 and the monolayers were formed after culturing for 21 days post confluence. The integrity of the cell monolayer was routinely evaluated by measuring transepithelial electrical resistance (TEER) and by quantifying the transfer of a 100 μM solution of phenolsulfonphthalein (phenol red) as described by Pereira-Caro et al.[11] Monolayers with a TEER ≥ 500 Ωcm^2 and phenol red transport <0.1% of phenol were considered suitable for use.

Nitrocatechols metabolism experiments. Two mL of nitrocatechols test solutions (100 μM; 0.1% DMSO) were apically added to each well. Control and treated cells were incubated at

154 37°C for 1, 2 and 4 h. Media and cytoplasmatic contents were separately subjected to HPLC
155 and LC-MS analyses. All metabolic experiments were repeated six times.
156 Nitrocatechols transport experiments. Two mL of the test solutions were added to the apical
157 or basolateral side to measure the apical-to-basolateral or basolateral-to-apical permeability,
158 respectively, while the contrary side was filled with the same volume of serum-free DMEM
159 with 0.1% DMSO and 500 μM of ascorbic acid. Media was analysed by HPLC after incubation
160 during 1, 2 and 4 h in a humidified atmosphere of 5% CO_2 at 37°C. The apparent permeability
161 coefficient (P_{app}, cm/s) and absorption rate (AR) were determined as described by Pereira-Caro
162 et al.[11] All transport experiments were repeated six times.
163
164 **Metabolism experiments in HepG-2 cells**
165 HepG2 cells were seeded in 6 cm diameter plates at a density of 2.5-3.0 x 10^6 cells/plate. Three
166 mL of nitrocatechols test solutions (100 μM; 0.1% DMSO) were added to each plate and
167 incubated at 37°C for 2 h (short-term) or 18 h (long-term). Media and cytoplasmic contents
168 were separately subjected to HPLC-DAD and LC-MS analyses. All metabolic experiments were
169 repeated three times.
170
171 **HPLC analysis**
172 All extracellular culture media and cell lysates from experiments carried out with Caco-2 and
173 HepG2 cells were analyzed by HPLC using an Agilent 1200 and an Agilent 1100 Liquid
174 Chromatographic System, respectively, both equipped with diode array UV-Vis detector and a
175 thermostatic autosampler (4°C, 50 μL injection volume). For separation a 250 mm x 4.6 mm
176 i.d., 4 μm particle size Superspher 100 RP18 column preceded by a Tracer C-160K1 holder with
177 an ODS precolumn was used in both cases. Elution of samples was performed at a flow rate of
178 1.0 mL/min at 37°C using as mobile phase 1% formic acid in deionized water (solvent A) and
179 acetonitrile (solvent B). The solvent gradient changed according to the following conditions:

from 95 to 90% A in 5 min; 85% A in 15 min; 80% A in 5 min; 75% A in 5 min; 70% A in 5 min, returning to initial conditions in 5 min (95% A) and followed by 5 min of maintenance. Chromatograms were acquired at 280 nm. Standards of the parent compounds were prepared in serum-free culture media in a range of concentrations from 1.25 μM to 100 μM obtaining a linear response for all standard curves, as checked by linear regression analysis with R^2 values greater than 0.99 (n=6). Metabolites were quantified as equivalents of the respective parent molecules. The different equipments used to evaluate samples from experiments with Caco-2 and HepG2 cells led to different retention times of common metabolites, in spite of conducting analysis with identical conditions (eluents, column, flow rate, gradient, etc.).

Mass spectrometry

An Agilent 1100 series liquid chromatograph/mass selective detector equipped with a DAD detector and a quadrupole mass spectrometer (Agilent Technologies) was used. Chromatographic conditions (eluents, column, flow rate, gradient, etc.) were the same as described above. Eluent flow (1 mL/min) was split 8:1 between the DAD detector and the MS ion source. The MS was fitted to an atmospheric pressure electrospray ionization (ESI) source, operated in negative ion mode. The electrospray capillary voltage was set to 3000 V, with a nebulizing gas (nitrogen) flow rate of 12 L/h and a drying gas temperature of 300°C. Data were acquired in scan mode (mass range *m/z* 100-900) at a scan rate of 1.5 s.

Identification of nitrohydroxytyrosyl conjugates

In vitro conjugation of nitroderivatives of HT was carried out using pure enzyme (catechol-*O*-methyltransferase, COMT) or a rat liver microsomal fraction that contained UDP-glucuronosyltransferase,[22] providing methyl and glucuronidated derivatives of the three nitrocatechols. In parallel, to complete the identification of nitrohydroxytyrosyl conjugates, media and cell fractions after metabolism experiments with Caco-2 and HepG2 cells were

incubated with β-glucuronidase/sulfatase to hydrolyze conjugated metabolites (glucuronides and/or sulfates).[22] All samples from in vitro conjugation and hydrolysis reactions were analyzed by HPLC-DAD (Agilent 1200 and Agilent 1100) and LC-MS analyses.

Statistical analysis

Statistical analyses were carried out using the program SPSS (version 19.0, SPSS, Inc., IBM Company). Data were studied using a one-way analysis of variance (ANOVA). The significance level was set at $p<0.05$. Data were given as mean ± standard deviation.

Results

Stability evaluation and cytotoxic effect of HT-nitroderivatives

We tested the efficiency of different concentrations of ascorbic acid (300, 500 and 1000 μM) protecting HT-nitroderivatives (100 μM in serum-free culture medium) from oxidation after incubation for 24 h at 37 ^{o}C in the absence of cells. A 300 μM ascorbic acid concentration did not confer full protection; however, NO_2HT, NO_2HT-A and NO_2HT-E were stable when incubated with 500 μM ascorbic acid (>98% recovery) (data not shown). This concentration of antioxidant was used in subsequent experiments (pH 7.2).

In addition, no cytotoxic effects were observed after incubation of 100 μM of HT-nitroderivatives with Caco-2 and HepG2 cells (data not shown).

Identification of metabolites of HT-nitroderivatives

HPLC analysis of cell culture media collected after incubation of HT-nitroderivatives with Caco-2 and HepG2 cells showed in both cases a number of additional peaks with absorbance at 280 nm that were not present in the culture medium, concomitant with a decrease of the parent compounds (Figures 2 and 3). These observations suggested that the additional peaks were

nitrocatechol metabolites. Subsequently, different approaches were used to determine the structure of these metabolites: analysis and confirmation of structures by electrospray ionization mass spectrometry in negative ion mode with selected ion monitoring (SIM); hydrolysis with β-glucuronidase/sulfatase; and in vitro conjugation of pure standards and comparison of retention times (RT) and spectral characteristics with test samples. It is worth noting that the different equipments used for experiments with Caco-2 and HepG2 cells, Agilent 1200 Series and Agilent 1100 Series Liquid Chromatographic System, respectively, resulted in slightly different retention times (RT) in common metabolites identified in both experiments.

Identification of nitrohydroxytyrosol (NO_2HT) conjugates. After incubation of NO_2HT with Caco-2 cells six new peaks were detected at RT of 9.1, 9.3, 10.0, 14.0, 21.0 and 24.4 min (labeled M1, M2, M3, M4, M5 and M6, respectively) (Figure 2). Peaks M1, M2, M3 and M4 exhibited a shift of the UV absorption maximum to shorter wavelengths (hypsochromic effect) (Table 1), while M5 and M6 hardly changed regarding NO_2HT. Peaks M1, M2, M3 and M4 disappeared after β-glucuronidase/sulfatase treatment with the subsequent increase of compound NO_2HT and peaks M5 and M6. In parallel, in vitro glucuronidation of NO_2HT yielded two peaks coincident in RT and spectroscopic characteristics with M1 and M2. LC-MS analysis showed a quasimolecular ion $[M-H]^-$ at *m/z* 374 for both peaks and fragment ion at *m/z* 198, corresponding to NO_2HT (Table 1). Chromatographic peaks M3 and M4 provided an $[M-H]^-$ ion at *m/z* 388 plus fragment ions at *m/z* 374, 212 and 198 corresponding to the loss of methyl, glucuronide and methylglucuronide moieties, respectively. All results allowed identifying M1 and M2 as NO_2HT monoglucuronides and M3 and M4 as NO_2HT methylglucuronides.

Identification of M5 and M6 at 21.0 and 24.4 min, respectively, was assessed by comparing the spectral characteristics and RT with those obtained biosynthetically after incubation of NO_2HT with COMT (data not shown), in addition to their LC-MS analysis ($[M-H]^-$ at *m/z* 212 plus

256 fragment ion at *m/z* 198 corresponding to NO_2HT). All these results allowed confirming the
257 identity of M5 and M6 as methyl conjugates of NO_2HT.
258 These six metabolites (M1-M6) were also identified in samples generated after incubation of
259 NO_2HT with HepG2 cells (Figure 3), although slight differences in RT in comparison with Caco-2
260 cells were observed as mentioned above (Table 1). Additionally, a chromatographic peak at 7.1
261 min labeled as M12, was detected, which showed a UV spectrum with λ_{max} at 290, shifted to
262 shorter wavelengths in line with NO_2HT monoglucuronides, and disappeared completely after
263 β-glucuronidase/sulfatase treatment. This observation along with the peak's fragmentation
264 pattern after LC-MS analysis ($[M-H]^-$ at *m/z* 550 and two fragment ions at *m/z* 374 and 198
265 corresponding to monoglucuronide of NO_2HT and free NO_2HT, respectively) allowed its
266 unambiguous identification as the NO_2HT diglucuronide.
267 Identification of nitrohydroxytyrosyl acetate (NO_2HT-A) conjugates. Incubation of NO_2HT-A
268 with Caco-2 and HepG2 cells was almost coincident with that derived from NO_2HT metabolism.
269 Metabolites M1-M6 were present after incubation of NO_2HT-A with Caco-2 cells (Figure 2), and
270 metabolites M1-M6 and M12 were formed after incubation with HepG2 cells (Figure 3).
271 Furthermore, a chromatographic peak at 26.6 min (labeled as M7) with a maximum at 292 nm
272 and a shoulder at 342 nm was detected in the studies with Caco-2 cells (Figure 2). Its LC-MS
273 analysis ($[M-H]^-$ ion at *m/z* 416 and fragment ion at *m/z* 240 after the loss of a glucuronide
274 moiety) was compatible with the enzymatic hydrolysis suffered after treatment with β-
275 glucuronidase/sulfatase, permitting its identification as NO_2HT-A monoglucuronide.
276 Identification of ethyl nitrohydroxytyrosyl ether (NO_2HT-E) conjugates. Four new peaks (M8,
277 M9, M10 and M11) were formed after incubation of the ethyl derivative (NO_2HT-E) with Caco-
278 2 and HepG2 cells (Figures 2 and 3). UV spectra of peaks M8, M9, M10 and M11 showed a
279 hypsochromic effect in comparison with their precursor NO_2HT-E. All metabolites disappeared
280 after enzymatic hydrolysis with β-glucuronidase/sulfatase. LC-MS analysis provided, in addition
281 with the corresponding quasimolecular ion, a fragment ion at *m/z* 226 for peaks M8 and M9,

and *m/z* 240 for peaks M10 and M11, generated after the loss of a glucuronide moiety (Table 1). These results allowed identifying M8 and M9 as NO_2HT-E monoglucuronides and M10 and M11 as methylglucuronide conjugates of NO_2HT-E.

Additionally, a chromatographic peak at 19.2 min labeled as M13, was detected after incubation of NO_2HT-E with HepG2 cells, which showed a UV spectrum with λ_{max} at 288, shifted to shorter wavelengths in line with NO_2HT-E monoglucuronides; this peak disappeared completely after β-glucuronidase/sulfatase treatment. These results, in addition to its fragmentation pattern after LC-MS analysis (Table 1) allowed its unambiguous identification as the NO_2HT-E diglucuronide.

Transepithelial transport of nitrocatechols through differentiated Caco-2 cell monolayers

Transport of nitrocatechols across Caco-2 monolayers was evaluated in independent experiments after calculating apical (AP) to basolateral (BL) and their BL to AP transport rates.[20] The apparent permeability coefficients (Papp, cm/s) were also calculated (Table 2). AP to BL transport was higher than BL to AP, resulting in absorption rate (AR) values higher than 1.0 (Table 2). These results show a high permeability of nitrocatechols across Caco-2 monolayers. In addition, the acetate and the ethyl ether derivatives showed higher AR values than their precursor, NO_2HT. In this manner, a direct relationship was observed between the lipophilicity of the three compounds and their AR values.

Quantitative analyses of nitrocatechols and their metabolites in Caco-2 cells

Time-dependent transport was observed up to 4 h (Figure 4). The percentage of compounds (metabolized plus non-metabolized) absorbed across Caco-2 monolayer after 4 h was higher for NO_2HT-A and NO_2HT-E (50.1% and 52.6% respectively, Figure 4B) than for their precursor NO_2HT (30.0%), in agreement with the higher AR described for the more lipophilic compounds (NO_2HT-A and NO_2HT-E) compared to NO_2HT.

Regarding the absorbed fraction of nitrocatechols, 80.6% of NO_2HT remained unmetabolized after 2 h, whereas the most lipophilic compounds, acetate and ethyl ether, were more extensively metabolized and only 17.3 and 33.0%, respectively, remained unchanged. It is worth noting that the major metabolite of NO_2HT-A, identified in the BL compartment corresponded to the product generated after its hydrolysis (NO_2HT), which in turn mostly remained unconjugated by phase II enzymes. Adding the hydrolyzed, unmetabolized compounds by phase II enzymes action (NO_2HT-A and NO_2HT), the fraction absorbed by Caco-2 cells which remained unmetabolized would reach 71.2% for NO_2HT-A, which is in line with the 80.6% quantified for NO_2HT. Regarding the nature of the metabolites identified, most were glucuronides and to a lower extent methylglucuronides and methyl conjugates (Figures 4A and 4B).

Quantitative analyses of nitrocatechols and their metabolites in HepG2 cells

The amount of unmetabolized parent compounds and their metabolites in the extracellular culture medium was quantified after 2 and 18 h of incubation with HepG2 cells. Differences were observed due to the incubation time as well as the chemical structure of each assayed compound. Results are summarized in Figure 5.

The percentage of unmetabolized compounds detected in the culture medium after 2 h of incubation with nitrocatechols represented 100, 60.6 and 97.3% for NO_2HT, NO_2HT-A and NO_2HT-E, respectively. These results point to a low uptake and metabolization of these compounds by HepG2 cells at short incubation times. The relatively higher metabolization of NO_2HT-A is a consequence of the hydrolysis that this molecule suffers to yield its precursor, since the remaining 39.4% corresponded to unconjugated NO_2HT. However, phase II derived metabolites were not identified after incubation of NO_2HT and NO_2HT-A with phase II enzymes. On the contrary, NO_2HT-E generated glucuronide conjugates, which represented 2.7% of the total compound in the cell culture medium.

In contrast, after 18 h of incubation, the metabolism was substantially high so that only 11.9 and 6.3% of the parent NO_2HT, and NO_2HT-E, respectively, were detected unmetabolized in the culture medium (Figure 5), while NO_2HT-A was completely transformed by HepG2 cells. The three compounds (NO_2HT, NO_2HT-A and NO_2HT-E) were transformed by phase II enzymes UDP-glucuronosyltransferase and COMT, generating mainly glucuronides, in addition to methyl and/or methylglucuronide conjugates. The extensive hydrolysis of the acetyl group present in NO_2HT-A yielding NO_2HT, unlike the ethyl ether derivative NO_2HT-E, marked the main difference between both lipophilic compounds. NO_2HT-E was extensively glucuronidated (72.0%,) while NO_2HT and NO_2HT-A were glucuronidated to a similar proportion (56.0% and 57.1%, respectively). These two compounds showed identical percentage of methylation (1.5%), in contrast to NO_2HT-E with no monomethyl conjugates detected (Figure 5).

Discussion

Nitrocatechols are a new class of bioactive compounds that may play a role against Parkinson disease (PD) due to their capacity to inhibit COMT enzyme.[2,3] European Food Safety Authority (EFSA) has recently issued a claim on the beneficial health effects of the phenolic fraction in virgin and/or extra virgin olive oil in association with its capacity to protect low-density lipoproteins (LDL) from oxidation.[23] Therefore, phenols naturally present in olive oil have turned into interesting substrates and further applications with extended potential health benefits have been explored. Thus, nitroderivative forms of HT and hydroxytyrosyl acetate (HT-A), in addition to a synthetic hydrophobic derivative of HT, ethyl hydroxytyrosyl ether (HT-E), have been synthesized in order to obtain new compounds with a higher and safer therapeutic profile than that of the nitrocatechols currently used to treat PD.[9,10] To better understand the biological activity of NO_2HT, NO_2HT-A and NO_2HT-E, it is essential to study their absorption and metabolism. This objective has been approached in the present study using human cell models.

Bioavailability of HT and its derivatives is high, with around 66% of the ingested dose absorbed from the small intestine,[24] and plasma concentrations as high as 40 μM after the intake of polyphenol-rich olive oil (containing 366 mg/kg).[25] Considering these findings and the pharmacological approach of the present study, focused in offering new bioactive compounds to ameliorate neurodegenerative diseases, the doses of nitrocatechol tested in the present study (100 μM) can be considered almost physiological.

In the present study, human epithelial colorectal adenocarcinoma cells (Caco-2) were differentiated by the conventional symmetric protocol (serum-containing medium in both apical and basolateral compartments). Recently, an alternative method for differentiating Caco-2 cells into enterocytes has been proposed, requiring serum only in basolateral medium (asymmetric protocol).[26] This is a more ethically and economically friendly procedure that presents advantages to be considered in future studies. Incubation of the tested nitrocatechols in human Caco-2 cells monolayers as an intestinal barrier model showed that the three compounds were efficiently absorbed. In addition, there was a direct relationship between their lipophilicity and absorption rate (AR), showing the importance of the hydrocarbon chain on their bioavailability; however, it is interesting noting that no differences in AR values were observed between acyl (NO_2HT-A) and alkyl (NO_2HT-E) derivatives. This behavior is in line with that described for their respective precursors (HT, HT-A and HT-E).[11,27] HT showed the same AR (1.1 ± 0.2) than NO_2HT, pointing out that the nitro functional group does not modify the bioavailability of the compound at intestinal level. Furthermore, a higher absorption of hydroxytyrosyl alkyl ethers and HT-A compared to HT was observed (with AR values 1.1-1.7-fold higher), with no differences between acyl and alkyl derivatives with the same hydrocarbon chain length (ethyl hydroxytyrosyl ether *vs* hydroxytyrosyl acetate) in agreement with the results described for HT-nitroderivatives. Previous studies have shown the same correlation between intestinal absorption and lipophilicity. Tammela et al.[28] described the influence of the alkyl chain length on the uptake and transport of synthetic alkyl gallates, being medium chain

386 length gallates (*n*-propyl) more quickly absorbed than the shorter derivatives (methyl) in Caco-
387 2 cells. In addition, Werdenberg et al.[29] described inverse absorption of fumaric acid esters
388 (methyl, ethyl, *n*-propyl, and *n*-pentyl) across Caco-2 cell monolayers as the alkyl ester chain
389 length increased.
390 After incubation with Caco-2 cells, the metabolites identified for nitroderivative compounds
391 (NO_2HT, NO_2HT-A and NO_2HT-E) were glucuronide, methylglucuronide and methyl derivatives.
392 It is noteworthy that alkyl derivative (NO_2HT-E) did not undergo hydrolysis to yield free NO_2HT
393 in contrast to the acyl one (NO_2HT-A) that was almost completely hydrolyzed by cellular
394 carboxylesterase to NO_2HT, which was subsequently conjugated by phase II enzymes. Similar
395 behavior has been observed for HT and its acyl and alkyl derivatives.[11,27]
396 The present work evidences that methylation was greatest for NO_2HT whereas glucuronidation
397 was greatest for NO_2HT-E, the most lipophilic compound. This outcome may be associated
398 with the fact that UDP-glucuronosyltransferases (UGTs) are a family of membrane-bound
399 proteins in the endoplasmic reticulum[30] being more accessible for lipophilic compounds. In
400 contrast, catechol-*O*-methyltransferase (COMT) is a cytosolic enzyme,[31] which would justify the
401 higher yield of methyl derivatives from NO_2HT, the most hydrophilic compound.
402 The proportions of unconjugated compounds reaching the basolateral compartment after 2 h
403 of incubation were 81, 71 and 33% for NO_2HT, NO_2HT-A and NO_2HT-E, respectively, considering
404 for NO_2HT-A the sum of unconjugated NO_2HT-A and NO_2HT. Since NO_2HT-A had a higher AR
405 value than NO_2HT (1.4 ± 0.1 *vs* 1.1 ± 0.2, respectively), these results indicate that the
406 transformation into the acetylated derivative is an interesting and easy way to improve the
407 bioavailability of NO_2HT. Furthermore, a significant proportion of nitrocatechols (NO_2HT,
408 NO_2HT-A and NO_2HT-E) may appear in non-conjugated forms in peripheral blood and reach
409 organs such as the liver.
410 In an attempt to understand the complete biotransformation of the absorbed nitrocatechols,
411 their uptake and metabolism was studied using HepG2 cells. The results revealed that after 18

412 h of incubation, extensive uptake and metabolism in HepG2 cells took place, thus supporting
413 that most conjugation reactions occur in the liver.[32]
414 Certain similarities with the results obtained from the intestinal metabolism (experiments with
415 Caco-2 cells) were observed after incubation with hepatic HepG2 cells. Glucuronidated
416 derivatives, followed by methylglucuronides and methyl derivatives were identified after
417 nitrocatechols (NO_2HT, NO_2HT-A and NO_2HT-E) metabolism by HepG2, whereas no sulfated
418 forms were detected. Ethyl ether derivative (NO_2HT-E) was not hydrolyzed to free NO_2HT, in
419 contrast to the acetate (NO_2HT-A), although NO_2HT-E was extensively conjugated into
420 glucuronide and methylglucuronide metabolites. These are more lipophilic compounds than
421 those derived from NO_2HT, and thus more likely to reach lipophilic targets. Attending to these
422 results, the lipophilic nature of compounds determined the proportion of generated
423 metabolites, the highest glucuronidated derivative contents corresponded to NO_2HT-E and the
424 highest methyl conjugates to NO_2HT. These results are in agreement with the location of phase
425 II enzymes in the cells as previously discussed.
426 Results on the bioavailability of HT nitroderivatives (NO_2HT, NO_2HT-A and NO_2HT-E) in HepG2
427 cells are in agreement with those of HT and its lipophilic derivatives, acyl and alkyl
428 derivatives.[12,22] A high metabolization yield was described for these compounds, as well as the
429 absence of hydrolysis of the alkyl derivatives (methyl, ethyl, propyl and butyl hydroxytyrosyl
430 ether), in contrast to the acyl derivative (HT-A), together with extensive formation of phase II
431 metabolites, except for sulfate derivatives.
432 All compounds detected in the cell lysates were below the limit of quantification, indicating
433 that no intracellular accumulation of nitrocatechols in colonic and hepatic cells occurred.
434 Considering the extensive hepatic metabolism described for nitroderivatives of HT (NO_2HT,
435 NO_2HT-A and NO_2HT-E), in agreement with numerous publications on olive oil phenols and
436 other flavonoids, the metabolic biotransformation may profoundly affect their biological
437 activity.[33,34] In this sense, the in vitro antioxidant activity of HT and its major metabolites were

comparatively evaluated in red blood cells.[35] HT had a higher activity compared to the glucuronidated derivatives, which showed limited activity preventing hemolysis of the red blood cells. Likewise, other in vitro studies have shown higher activity for quercetin than its glucuronidated derivative, the most abundant metabolite identified in blood.[36] Although in vitro results may be far from what occurs in vivo, it has been postulated that the in vivo conjugation/deconjugation cycle is a reversible process that would explain the formation of the parent aglycon and the biological activity of some polyphenols.[36] Recently, Rubio et al.[37] described in rats a decreasing trend of the conjugated forms of HT, parallel to increasing free HT up to 6 h in red blood cells after the ingestion of a phenolic rich extract obtained from alperujo, suggesting intracellular hydrolysis of HT conjugates. Similarly, the extensive hepatic metabolism of the nitrocatechols generating glucuronide, methyl and methylglucuronide conjugates will partially or completely block the *ortho*-diphenolic group. Therefore, their remarkable COMT inhibitory effects in the brain,[14,15] should involve the hydrolysis of nitrocatechol conjugates, key for their activity as COMT inhibitors.

In summary, nitrocatechols are efficiently absorbed and partially metabolized in Caco-2 cells. Much of the absorbed compounds were not metabolized and could reach other organs such as the liver in the parent form. In HepG2 cells, nitrocatechols are extensively uptaken and metabolized. There is a direct relationship between the lipophilic nature of the compound and its uptake and biotransformation. NO_2HT-A was extensively hydrolyzed into NO_2HT, in contrast to NO_2HT-E, which remained unhydrolyzed. The main metabolites detected after metabolism in Caco-2 and HepG2 cells were glucuronides, methyl derivatives and methylglucuronides, but not sulfated derivatives.

Funding

This work was supported by Grant P09-AGR-5098 from Junta de Andalucía (Spain). E.G. thanks Junta de Andalucía for a predoctoral fellowship.

The authors declare no competing financial interests.

464 **References**

465 1. Prince, M.; Bryce, R.; Albanese, E.; Wimo, A.; Ribeiro, W.; Ferri, C. P. The global prevalence
466 of dementia: a systematic review and metaanalysis. *Alzheimers Dement.* **2013**, *9*, 63-75 e2.
467 2. Gordin, A.; Kaakkola, S.; Teravainen, H. Clinical advantages of COMT inhibition with
468 entacapone — a review. *J. Neural Transm.* **2004**, *111*, 1343–1363.
469 3. Bonifácio, M. J.; Palma, P. N.; Almeida, L.; Soares-da-Silva, P. Catechol-O-methyltransferase
470 and its inhibitors in Parkinson's disease. *CNS Drug Rev.* **2007**, *13*, 352–379.
471 4. Forsberg, M. M.; Huotari, M.; Savolainen, J.; Männistö, P. T. The role of physicochemical
472 properties of entacapone and tolcapone on their efficacy during local intrastriatal
473 administration. *Eur. J. Pharm. Sci.* **2005**, *24*, 503-11.
474 5. Learmonth, D. A.; Bonifácio, M. J.; Soares-da-Silva, P. Synthesis and biological evaluation of
475 a novel series of "*ortho*-nitrated" inhibitors of catechol-*O*-methyltransferase. *J. Med. Chem.*
476 **2005**, *48*, 8070–8078.
477 6. Pereira-Caro, G.; Mateos, R.; Sarria, B.; Cert, R.; Goya, L.; Bravo, L. Hydroxytyrosyl acetate
478 contributes to the protective effects against oxidative stress of virgin olive oil. *Food Chem.*
479 **2012**, *131*, 869-878.
480 7. Mateos, R.; Pereira-Caro, G.; Bacon, J. R.; Bongaerts, R.; Sarria, B.; Bravo, L.; Kroon, P. A.
481 Anticancer Activity of Olive Oil Hydroxytyrosyl Acetate in Human Adenocarcinoma Caco-2
482 Cells. *J. Agric. Food Chem.* **2013**, *61*, 3264-3269.
483 8. Tabernero, M.; Sarriá, B.; Largo, C.; Madrona, A.; Espartero, J. L.; Bravo, L.; Mateos, R.
484 Comparative evaluation of the cardio-metabolic effects of hydroxytyrosol and its lipophilic
485 derivatives (hydroxytyrosyl acetate and ethyl hydroxytyrosyl ether) in hypercholesterolemic
486 rats. *Food Funct.* **2014**, *5*, 1556-1563.
487 9. Trujillo, M.; Gallardo, E.; Madrona, A.; Bravo, L.; Sarriá. B.; González-Correa, J. A.; Mateos,
488 R.; Espartero, J. L. Synthesis and antioxidant activity of nitrohydroxytyrosol and its acyl
489 derivatives. *J. Agric Food Chem.* **2014**, *62*, 10297-10303.

10. Gallardo, E.; Palma-Valdes, R.; Sarriá, B.; Gallardo, I.; De la Cruz, J. P.; Bravo, L.; Mateos, R.; Espartero, J. L. Synthesis and antioxidant activity of alkyl nitroderivatives of hydroxytyrosol. Molecules **2015**, submitted.

11. Pereira-Caro, G.; Mateos, R.; Saha, S.; Madrona, A.; Espartero, J. L.; Bravo, L.; Kroon, P. A. Transepithelial transport and metabolism of new lipophilic ether derivatives of hydroxytyrosol by enterocyte-like Caco-2/TC7 cells. *J. Agric. Food Chem.* **2010**, *58*, 11501-11509.

12. Pereira-Caro, G.; Bravo, L.; Madrona, A.; Espartero, J. L.; Mateos, R. Uptake and metabolism of new synthetic lipophilic derivatives, hydroxytyrosyl ethers, by human hepatoma HepG2 cells. *J. Agric. Food Chem.* **2010**, *58*, 798-806.

13. Pereira-Caro, G.; Sarriá, B.; Madrona, A.; Espartero, J. L.; Goya, L.; Bravo, L.; Mateos, R. Alkyl hydroxytyrosyl ethers show protective effects against oxidative stress in HepG2 cells. *J. Agric. Food Chem.* **2011**, *59*, 5964-5976.

14. Gallardo, E.; Madrona, A.; Palma-Valdés, R.; Trujillo, M.; Espartero, J. L.; Santiago, M. The effect of hydroxytyrosol and its nitroderivatives on catechol-*O*-methyl transferase activity in rat striatal tissue. *RSC Advances* **2014**, *4*, 61086–61091.

15. Gallardo, E.; Madrona, A.; Palma-Valdés, R.; Espartero, J. L.; Santiago, M. Effect of intracerebral hydroxytyrosol and its nitroderivatives on striatal dopamine metabolism: A study by in vivo microdialysis. *Life Sci.* **2015**, *134*, 30–35.

16. Learmonth, D. A.; Palma, P. N.; Vieira-Coelho, M. A.; Soares da-Silva, P. Synthesis, Biological Evaluation and Molecular Modeling Studies of a Novel, Peripherally Selective Inhibitor of Catechol-*O*-Methyltransferase. *J. Med. Chem.* **2004**, *47*, 6207-6217.

17. Kambur, O.; Mannisto, P. T.; Pusa, A. M.; Kaenmaki, M.; Kalso, E. A.; Kontinen, V. K. Nitecapone reduces development and symptoms of neuropathic pain after spinal nerve ligation in rats. *Eur. J. Pain* **2011**, *15*, 732-740.

515 18. Sarriá, B.; Mateos, R.; Gallardo, E.; Ramos, S.; Martín, M. A.; Bravo, L.; Goya, L.
516 Nitroderivatives of olive oil phenols protect HepG2 cells against oxidative stress. *Food*
517 *Chem. Toxicol.* **2012**, *50*, 3752-3758.
518 19. FDA. Guidance for industry: Walver of in vivo Bioavailability and Bioequivalence Studies for
519 Immediate-Release Solid Oral Dosages Forms Based on a Biopharmaceutics Classification
520 System. US Food and Drug Administration, Center for Drug Evaluation and Research, USA,
521 2000.
522 20. Fardel, O.; Morel, F.; Ratanasanh, D.; Fautreel, A.; Beaune, P.; Guillouzo, A. Expression of
523 drug metabolizing enzymes in human HepG2 hepatoma cells. *Cell. Mol. Aspects Cirrhosis*
524 **1992**, *216*, 327-330.
525 21. Fernández-Bolanos, J.; Here dia, A.; Rodríguez, G.; Rodríguez, R.; Jiménez, A.; Guillén, R.
526 Methods for obtaining purified hydroxitirosol from products and by-products derived from
527 the olive tree. U.S. 6849,770 B2, **2005**.
528 22. Mateos, R.; Goya, L.; Bravo, L. Metabolism of the olive oil phenols hydroxytyrosol, tyrosol
529 and hydroxytyrosyl acetate by human hepatoma HepG2 cells. *J. Agric. Food Chem.* **2005**, *53*,
530 9897-9905.
531 23. EFSA Panel on Dietetic Products, Nutrition and Allergies. Scientific opinion on the
532 substantiation of health claims related to polyphenols in olive oil and protection of LDL
533 particles from oxidative damage. *EFSA J.* **2011**, *9*, 2033-2058.
534 24. Vissers, M. N.; Zock, P. L.; Roodenburg, A. J.C.; Leenen, R.; Katan, M. B. Olive oil phenols are
535 absorbed in humans. J. Nutr. 2002, 409-417.
536 25. Covas, M. I.; de la Torre, K.; Farre-Albaladejo, M.; Kaikkonen, J.; Fito , M.; Lopez-Sabater, C.;
537 Pujadas-Bastardes, M. A.; Joglar, J.; Weinbrenner, T.; Lamuela-Raventó s, R. M.; de la
538 Torre, R. Postpandrial LDL phenolic content and LDL oxidation are modulated by olive oil
539 phenolic compounds in humans. Free Radical Biol. Med. 2006, 40, 608-616.

26. Ferruzza, S.; Rossi, C.; Scarino, M.L.; Sambuy, Y. A protocol for differentiation of human intestinal Caco-2 cells in asymmetric serum-containing medium. Toxicol. In Vitro **2012**, *26*, 1252–1255.

27. Mateos, R.; Pereira-Caro, G.; Saha, S.; Cert, M.; Redondo-Horcajo, M.; Bravo, L.; Kroon P. A. Acetylation of hydroxytyrosol enhances its transport across differentiated Caco-2 cell monolayer. *Food Chem.* **2011**, *125*, 865-872.

28. Tammela, P.; Laitinen, L.; Galkin, A.; Wennberg, T.; Heczko, R.; Vuorela, H.; Slotte, J. P.; Vuorela, P. Permeability characteristics and membrane affinity of flavonoids and alkyl gallates in Caco-2 cells and in phospholipids vesicles. *Arch. Biochem. Biophys.* **2004**, *425*, 93-99.

29. Werdenberg, D.; Joshi, R.; Wolffram, S.; Merkle, H. P.; Langguth, P. Presystemic metabolism and intestinal absorption of antipsoriaticfumaric acid esters. *Biopharm. Drug Dispos.* **2003**, *24,* 259-273.

30. Turkey, R. H.; Strassburg, C. P. Human UDP-glucuronosyltransferases: metabolism, expression and disease. *Ann. Rev. Pharmacol. Toxicol.* **2000**, *40*, 581-616.

31. Tenhunen, J.; Salminen, M.; Lundstrom, K.; Kiviluoto, T.; Savolainen, R.; Ulmanen, I. Genomic organization of the human catechol-*O*-methyltransferase gene and its expression from two distinct promoters. *Eur. J. Biochem.* **1994**, *223*, 1049-1059.

32. D´Archivio, M.; Filesi, C.; Vari, R.; Scazzocchio, B.; Masella, R. Bioavailability of the Polyphenols: Status and Controversies. *Int. J. Mol. Sci.* **2010**, *11*, 1321-1342.

33. Day, A. J.; Bao, Y.; Morgan, M. R.; Williamson, G. Conjugation position of quercetin glucuronides and effect on biological activity. *Free Radic. Biol. Med.* **2000**, *29*, 1234-1243.

34. Wen, X.; Walle, T. Methylation protects dietary flavonoids from rapid hepatic metabolism. *Xenobiotica* **2006**, *36*, 387-397.

35. Paiva-Martins, F.; Silva, A.; Almeida, V.; Carvalheira, M.; Serra, C.; Rodrígues-Borges, J. E.; Fernandes, J.; Belo, L.; Santos-Silva, A. Protective activity of hydroxytyrosol metabolites on erythrocyte oxidative-induced hemolysis. *J. Agric. Food Chem.* **2013**, *61*, 6636-6642.

36. Perez-Vizcaino, F.; Duarte, J.; Santos-Buelga, C. The flavonoid paradox: conjugation and deconjugation as key steps for the biological activity of flavonoids. *J. Sci. Food Agric.* **2012**, *92*, 1822-1825.

37. Rubió, L.; Serra, A.; Maciá, A.; Piñol, C.; Romero, M. P.; Motilva, M. J. In vivo distribution and deconjugation of hydroxytyrosol phase II metabolites in red blood cells: A potential new target for hydroxytyrosol. *J. Funct. Foods*. **2014**, *10*, 139-143.

Table 1. Chromatographic and spectroscopic characteristics of nitrohydroxytyrosol (NO_2HT, **1**), nitrohydroxytyrosyl acetate (NO_2HT-A, **2**) and ethyl nitrohydroxytyrosyl ether (NO_2HT-E, **3**) and the metabolites formed after incubation with Caco-2 and HepG2 cells.

Compound	MW	RT(min) Caco-2	RT(min) HepG2	λ_{max} (nm)	$[M-H]^-$ (m/z)	Fragment ion (m/z)	Proposed structure
1	199	13.4	12.2	354, 308sh	198	150, 137	Nitrohydroxytyrosol (**1**)
2	241	32.9	30.3	354, 306sh	240	150	Nitrohydroxytyrosyl acetate (**2**)
3	227	36.2	33.8	354, 312sh	226	151	Ethyl nitrohydroxytyrosyl ether (**3**)
M1	375	9.1	9.3	330	374	198	Monoglucuronide of **1**
M2	375	9.3	10.2	290, 344sh	374	198	Monoglucuronide of **1**
M3	389	10.0	10.6	282, 332sh	388	374, 212, 198	Methylglucuronide of **1**
M4	389	14.0	13.2	292, 342sh	388	374, 212, 198	Methylglucuronide of **1**
M5	213	21.0	18.8	352, 306sh	212	198	Methyl conjugate of **1**
M6	213	24.4	21.3	354, 306sh	212	198	Methyl conjugate of **1**
M7	417	26.6	-	292, 342sh	416	240	Monoglucuronide of **2**
M8	403	29.2	27.5	292, 340sh	402	226	Monoglucuronide of **3**
M9	403	29.9	28.3	292, 344sh	402	226	Monoglucuronide of **3**
M10	417	31.0	29.7	326	416	240	Methylglucuronide of **3**
M11	417	32.2	30.5	286, 342sh	416	240	Methylglucuronide of **3**
M12	551	-	7.1	290, 328sh	550	374,198	Diglucuronide of **1**
M13	579	-	19.2	288	578	402, 226	Diglucuronide of **3**

MW: Molecular weight; RT: Retention time; $[M-H]^-$: Quasimolecular ion

Table 2. Apparent permeability coefficient (P_{app}, cm/s) and absorption rate (AR) values for nitrocatechols (nitrohydroxytyrosol (**1**), nitrohydroxytyrosyl acetate (**2**) and ethyl nitrohydroxytyrosyl ether (**3**))[a].

Compound	AP – BL (Papp, x 10^{-6} cm/s)	BL – AP (Papp, x 10^{-6} cm/s)	Absorption Rate (AR)
1	47.7 ± 0.8	44.1 ± 1.9	1.1 ± 0.1 [a]
2	75.3 ± 0.4	52.9 ± 0.1	1.4 ± 0.1 [b]
3	75.1 ± 0.3	48.8 ± 0.3	1.5 ± 0.2 [b]

[a] AP-BL indicates apical to basolateral transport; BL-AP indicates basolateral to apical transport; AR values are from P_{app} AP-BL/Papp BL-AP. Values are expressed as mean ± standard deviation of three determinations, where all values within a column with different letters are significantly different ($p < 0.05$).

Figure Captions

Figure 1. Chemical structure of nitroderivatives of hydroxytyrosol: (**1**) Nitrohydroxytyrosol (NO_2HT); (**2**) Nitrohydroxytyrosyl acetate (NO_2HT-A); (**3**) Ethyl nitrohydroxytyrosyl ether (NO_2HT-E).

Figure 2. Typical chromatographic profile at 280 nm of culture medium after incubation of nitrocatechols with Caco-2 cells for 4 h: NO_2HT (**1**) in the apical (A) and basolateral (B) compartments; NO_2HT-A (**2**) in the apical (C) and basolateral (D) compartments; and NO_2HT-E (**3**) in the apical (E) and basolateral (F) compartments. For peak identification see Table 1.

Figure 3. Typical chromatographic profile at 280 nm of culture medium after incubation of nitrocatechols with HepG2 cells after 18 h incubation. NO_2HT (**1**) (A); NO_2HT-A (**2**) (B); NO_2HT-E (**3**) (C). For peak identification see Table 1.

Figure 4. Percentage of nitrocatechols (**1**: NO_2HT; **2**: NO_2HT-A; **3**: NO_2HT-E) and their metabolites found in the apical (AP) and basolateral (BL) compartments after 1, 2, and 4 h of incubation with Caco-2 cells after apical loading of the parent compound (100 μM). (A) Percentage of parent compounds and types of metabolites in the apical side. (B) Percentage of parent compounds and types of metabolites in the basolateral side. Results showed a standard deviation <10%.

Figure 5. Percentage of nitrocatechols (**1**: NO_2HT; **2**: NO_2HT-A; **3**: NO_2HT-E) and their metabolites found in extracellular culture medium after 2 and 18 h of incubation of the parent compound (100 μM) with HepG2 cells.

Figure 1.

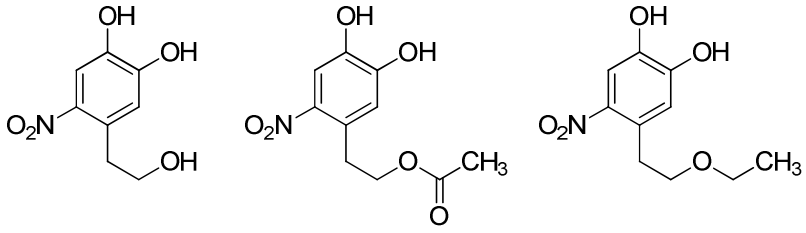

NO_2HT (**1**) NO_2HT-A (**2**) NO_2HT-E (**3**)

Figure 2

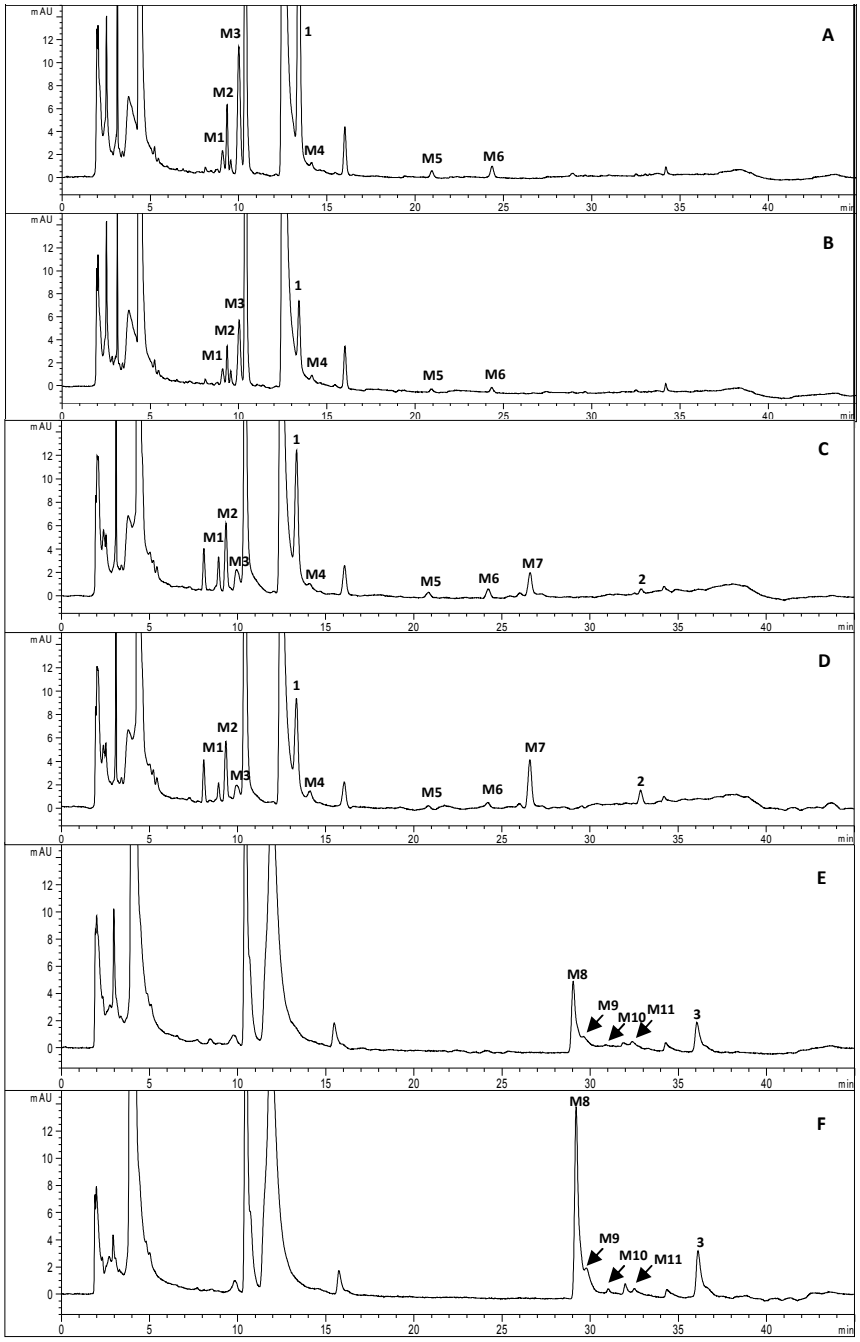

Figure 3

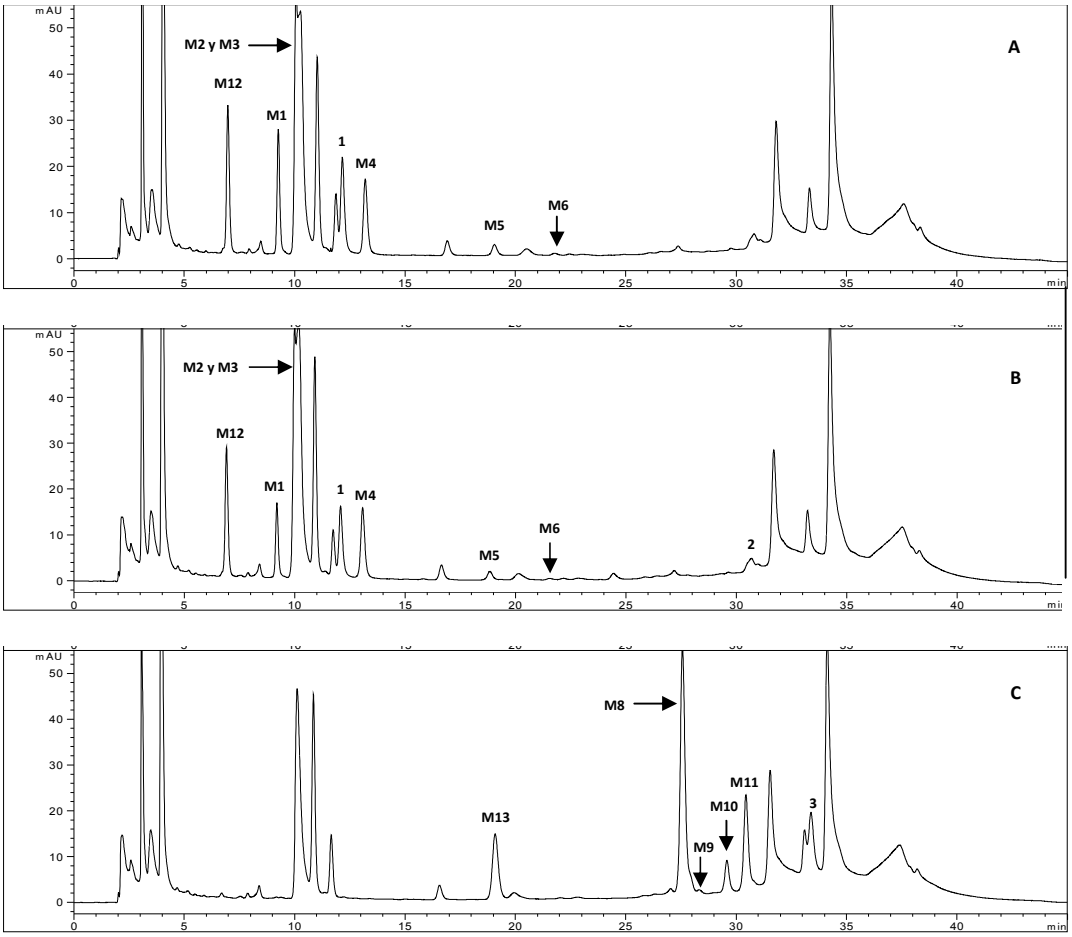
A
M2 y M3
M12
M1
1
M4
M5
M6
B
M2 y M3
M12
M1
1
M4
M5
M6
2
C
M8
M13
M9
M10
M11
3
mAU
min

Figure 4.

A) Apical Side

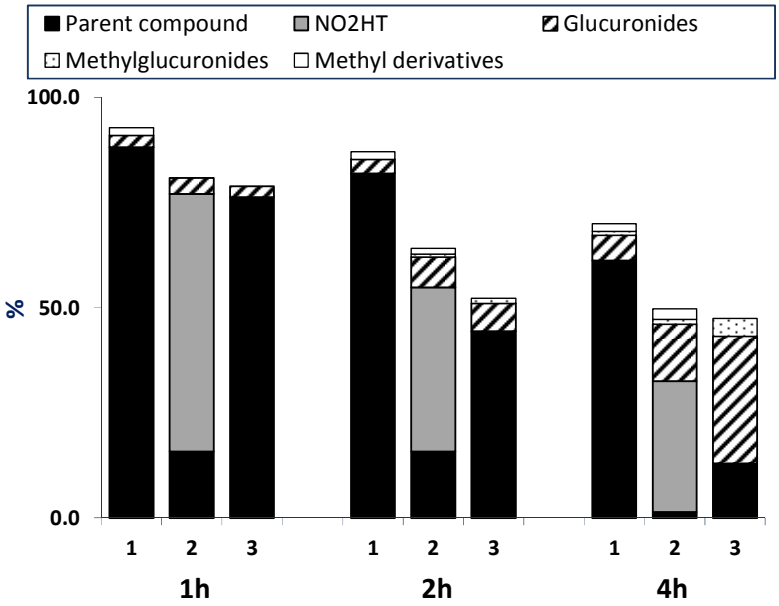

B) Basolateral Side

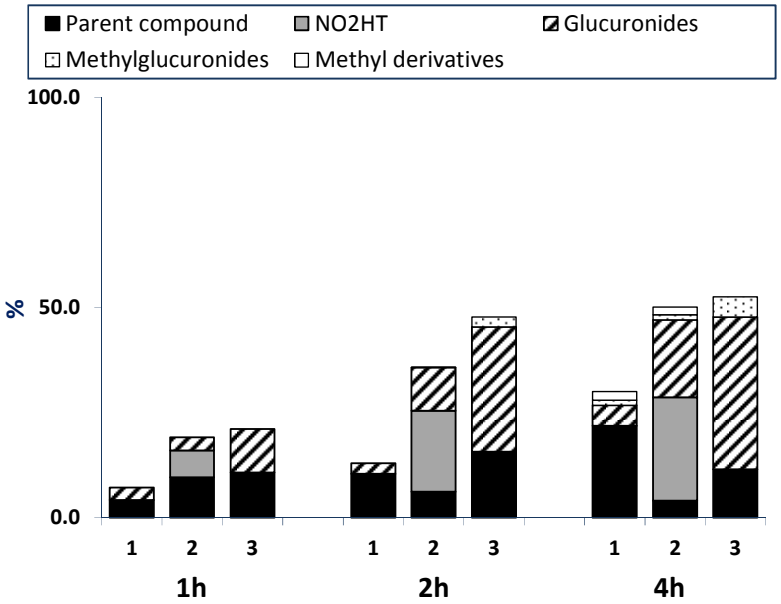

Figure 5.

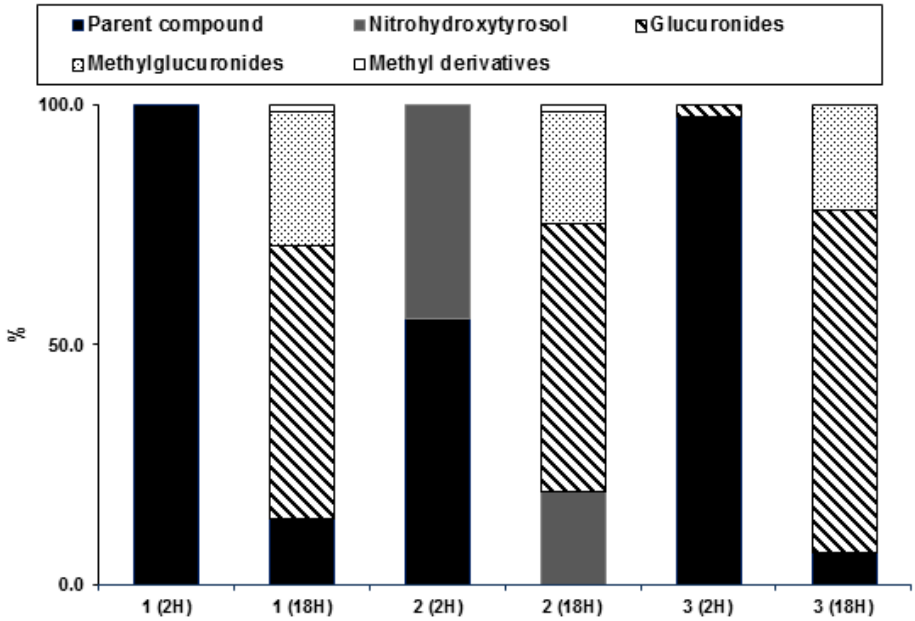
Parent compound
Nitrohydroxytyrosol
Glucuronides
Methylglucuronides
Methyl derivatives
100.0
50.0
0.0
%
1 (2H)
1 (18H)
2 (2H)
2 (18H)
3 (2H)
3 (18H)

TOC

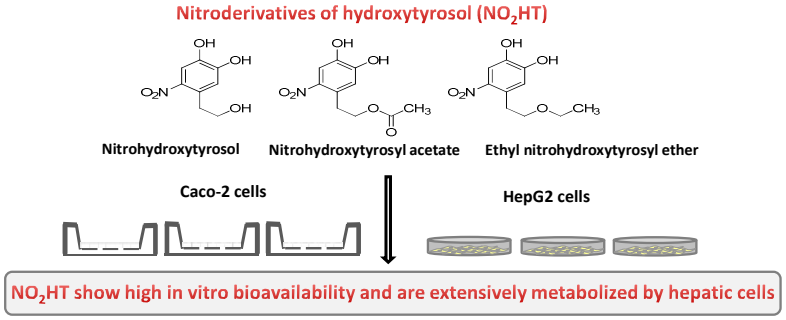
Nitroderivatives of hydroxytyrosol (NO_2HT)
Nitrohydroxytyrosol
Nitrohydroxytyrosyl acetate
Ethyl nitrohydroxytyrosyl ether
Caco-2 cells
HepG2 cells
NO_2HT show high in vitro bioavailability and are extensively metabolized by hepatic cells